A study of Sn-Bi-Ag-(In) lead-free solders

REN-KAE SHIUE*
Department of Materials Science and Engineering, National Dong Hwa University, Hualien 974, Taiwan, R.O.C.
E-mail: rkshiue@mail.ndhu.edu.tw

LEU-WEN TSAY
Institute of Materials Science and Engineering, National Taiwan Ocean University, Keelung 202, Taiwan, R.O.C.

CHUN-LUN LIN, JIA-LIN OU
Department of Materials Science and Engineering, National Dong Hwa University, Hualien 974, Taiwan, R.O.C.

Sn-Bi-Ag-(In) solder alloys have been extensively studied in the study. The experimental results reveals that the liquidus temperatures of Sn-(1–5) Bi-(2–3.5)Ag-(0–10)In solders are between 201.7 and 225.3°C, which were higher than that of the most popular eutectic Pb-Sn solder (183°C). Additions of (5–10) wt% In into Sn-Bi-Ag solders can effectively decrease the melting point of the solder alloy. However, the gap between T_s and T_L temperatures increases with the additions of Bi and In into Sn-Bi-Ag-(In) solders. Although there is no flux applied during soldering, most Sn-Bi-Ag-(In) solder alloys can well bond the Au/Ni metallized copper substrate. 94Sn-3Bi-3Ag solder demonstrates the lowest wetting angle of 45° among all test samples. Thermal expansion coefficients of both 94Sn-3Bi-3Ag and 90Sn-2Bi-3Ag-5In solders are slightly less than that of 63Sn-37Pb. Both 90Sn-2Bi-3Ag-5In/substrate and 94Sn-3Bi-3Ag/substrate interfaces demonstrate similar reaction kinetics in the experiment. The stability of the interface is greatly impaired during 90°C aging. Some locations of the electroless Ni layer break down, and new phases are formed nearby the interface during aging treatment. Initially, the growth of Ni-rich $(Ni,Cu)_3Sn_4$ phase dominates the interfacial reaction. However, the growth of Cu-rich $(Cu,Ni)_6Sn_5$ phase will dominate the reaction layer for specimens aged at 90°C for long time periods. © *2003 Kluwer Academic Publishers*

1. Introduction

Soldering and brazing are two primary methods for joining dissimilar materials [1–4]. Soldering is similar to brazing except that soldering employs a filler alloy with a liquidus below 450°C (840°F) [3]. The importance of soldering in the field of electronic packaging is increasing due to the rapid growth of the industry. Although the basic principles of soldering and brazing processes are the same, it is possible to distinguish soldering process in electronics as a separate subject [3]. Binary Sn-Pb alloys are extensively used in the electronics industry [5]. The melting point of binary Sn-Pb solders can be modified by changing Pb content in the alloy, e.g., 63Sn-37Pb, 60Sn-40Pb and 5Sn-95Pb, etc., so that Sn-Pb solders can be applied in manufacturing various electronic components [1]. Extensive literature is available which discusses the mechanical properties, physical properties, microstructural evolution at the soldered interface, corrosion resistance, etc of Sn-Pb solders [6–12]. However, legislation restricts and/or

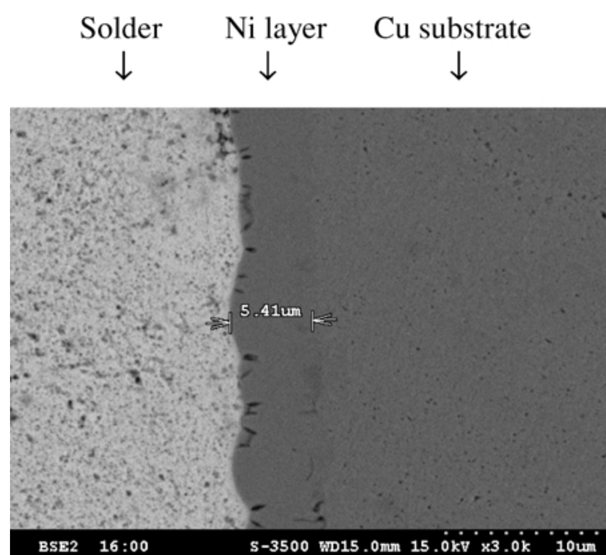

Figure 1 Cross sectional SEM BSE image of the solder alloy on Au/Ni metallized Cu substrate.

*Author to whom all correspondence should be addressed.

 © *2003 Kluwer Academic Publishers*

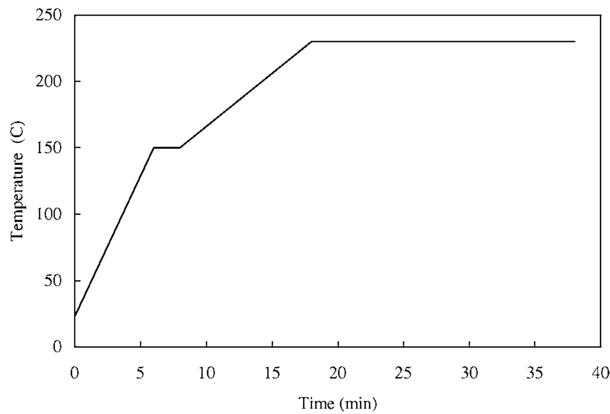

Figure 2 Thermal cycle of Sn-Bi-Ag-(In) alloys used in the experiment.

eliminates the use of Pb due to environmental and toxicological concerns, and the importance of lead-free solders is increasing in recent years [5, 13].

There are many Pb-free solders, e.g., Sn-Bi, Sn-In, Sn-Ag and Sn-Zn [5, 13–16]. It is also reported that the most promising Pb-free solders are tin-based multicomponent alloys with alloying elements such as Bi, In, Ag and Zn [17]. There are strict manufacturing and performance requirements for solder alloys used in electronic packaging [5]. Cost, mechanical, thermal, electrical, chemical and metallurgical properties of the

TABLE I DSC analysis of Sn-Bi-Ag-(In) solders

Alloy composition (wt%)	T_s (°C)	T_L (°C)
94Sn-3Bi-3Ag	206.4	225.3
85Sn-2Bi-3Ag-10In	193.1	209
94.5Sn-1Bi-2Ag-2.5In	202.8	222
81.5Sn-5Bi-3.5Ag-10In	180.1	201.7
89Sn-3Bi-3Ag-5In	190	215.5
90Sn-2Bi-3Ag-5In	194.7	215
84Sn-3Bi-3Ag-10In	193	206
87Sn-5Bi-3Ag-5In	191.7	209

solder alloy are important issues in the application of Pb-free solders. The solder alloy not only conducts the electrical current in the electronic packaging, but also dissipates heat generated from the chip into the substrate during operation [5, 13]. Meanwhile, the difference in thermal expansion coefficients between the Si chip and the substrate results in thermal stresses upon thermal cycling of the component during operation. The thermal fatigue behavior of solder joints plays an important role in determining the reliability of microelectronic components [18–22]. By increasing the packaging density of electronic components, the reliability of the packaging is strongly related to the solder alloys being used [13, 22]. Therefore, thermal properties, e.g., thermal expansion coefficients, solidus

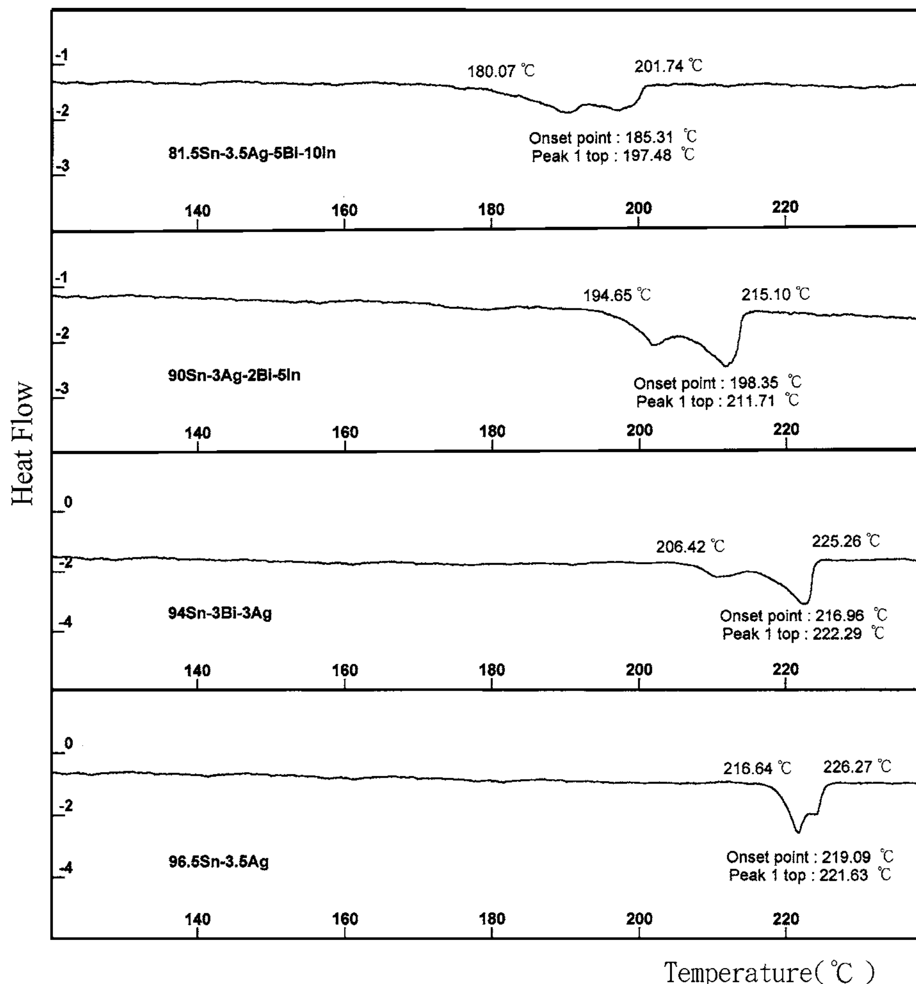

Figure 3 Endothermic profiles of selected Sn-Bi-(Ag)-(In) solders in the DSC analysis.

and liquidus temperatures of solder alloys, are important issues in evaluating the reliability of electronic components.

Traditionally, fluxes are used in most soldering processes. However, the removal of fluxes after soldering can be a potential problem in the modern packaging process. In addition to flux soldering of electronic components to copper substrates, there is an alternative way with no or less flux usage in soldering [23–25]. The copper substrate is firstly plated with a Ni layer, and subsequently plated with a thin layer of Au. With the aid of a thin Au protective layer on the Ni-plated Cu substrate, most solders can be successfully processed in air with no or mild flux. This Au/Ni metallization has become increasingly common in microelectronic packaging [23]. The surface Au layer can protect the Cu substrate from corrosion and oxidation, and the Ni layer provides a diffusion barrier to inhibit the detrimental growth of Cu-Sn Intermetallics [23, 26].

Sn-Bi based alloys are alternative choices to replace Sn-Pb solders. Some research works are available in the literature, but the knowledge of interfacial reaction kinetics of the solders on Au/Ni metallized Cu substrate is insufficient [27–32]. The purpose of this research

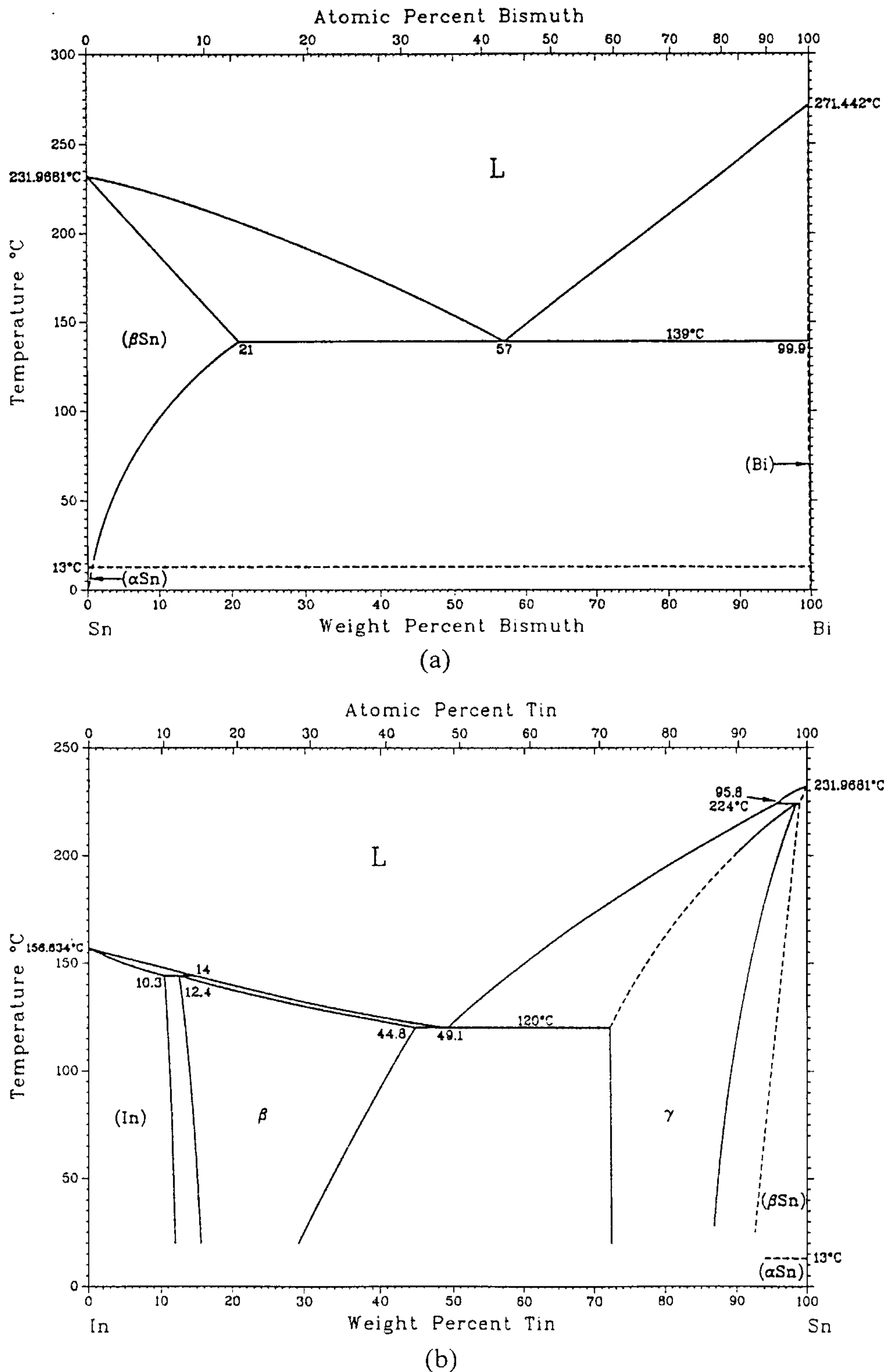

Figure 4 Related binary alloy phase diagrams in the study: (a) Sn-Bi, (b) Sn-In, (c) Sn-Ni and (d) Sn-Cu [35]. (*Continued*)

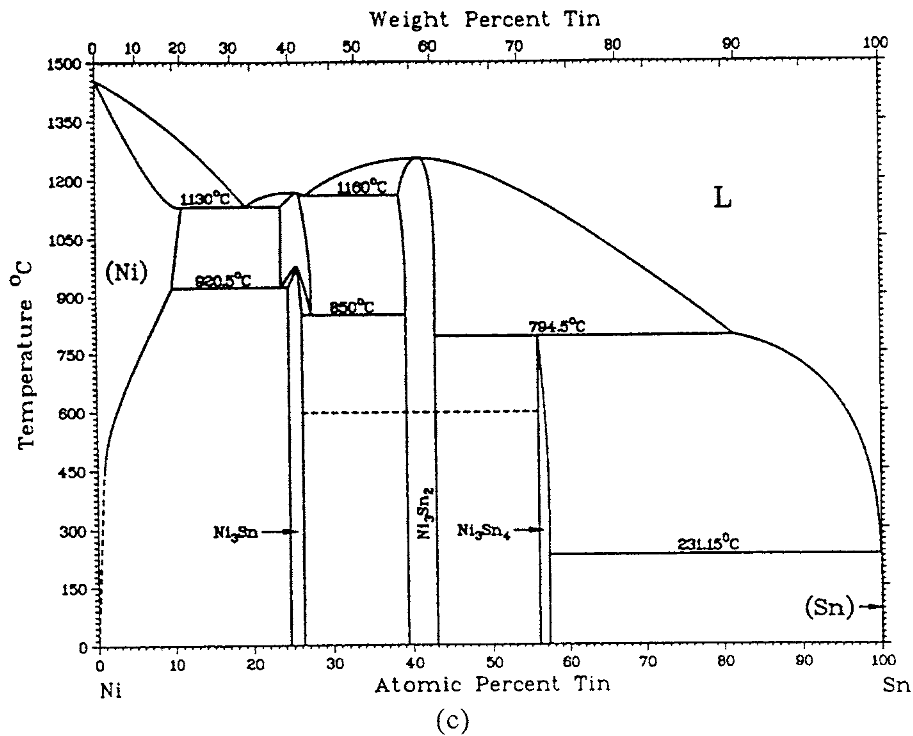

(c)

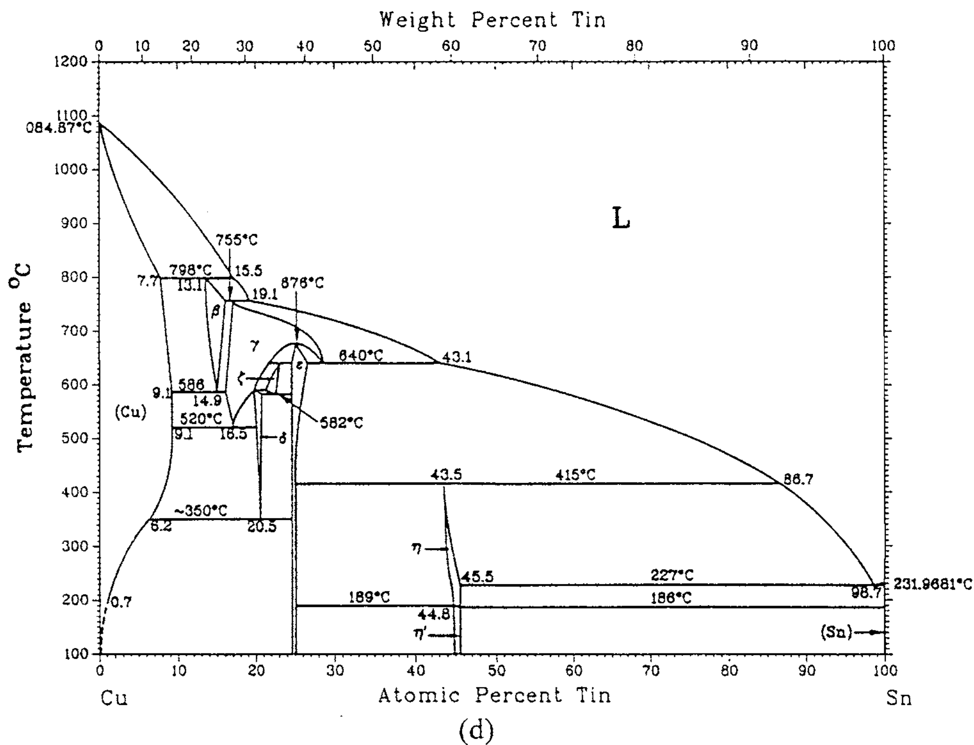

(d)

Figure 4 (*Continued*).

is to focus on Sn based lead-free solders with various amounts of Bi, Ag and In additions. The melting behavior, wetting characteristics, coefficient of thermal expansion (CTE), microstructure and interfacial reaction kinetics between the selected Sn-Bi-Ag-(In) solders and Au/Ni metallized Cu substrate are extensively studied.

2. Experimental procedures

The substrate material was high purity oxygen-free copper with 0.5 mm in thickness. It was first chemical plated by a Ni layer with a thickness of about 5.5 μm, and followed by a thin Au plating of less than 0.1 μm. Fig. 1 shows the cross section of an SEM backscattered electron (BSE) image of the solder alloy on a Au/Ni metallized Cu substrate. The disappearance of the thin Au layer can be attributed to the dissolution of Au atoms into the solder alloy during soldering. Many Sn-Bi-Ag-(In) solder alloys were studied using thermal analysis as displayed in Table I. Thermal analysis of the solder alloys was performed by SETARAM Labsys® DSC (Differential Scanning Calorimetry) and Setsys® TMA (Thermalmechanical Analysis) under the protection of 1 L/min Ar flow [33]. The heating rate for DSC analysis was set at 1°C/min between 25 and 250°C. The thermal

TABLE II Wetting angle measurements of Sn-Bi-Ag-(In) solders

Composition (wt%)	Bonding condition	Wetting angle
94Sn-3Bi-3Ag	Good	45°
90Sn-2Bi-3Ag-5In	Good	77°
81.5Sn-5Bi-3.5Ag-10In	Good	85°
87Sn-5Bi-3Ag-5In	Good	(liquation)

TABLE III Thermal expansion coefficients of three solder alloys

Composition (wt%)	Measured CTE (ppm/°C)	Averaged CTE (ppm/°C)
94Sn-3Bi-3Ag	24.1	24.0
	24.5	
	23.4	
90Sn-2Bi-3Ag-5In	23.7	24.0
	24.2	
	24.2	
63Sn-37Pb	25.0	25.8
	25.7	
	26.7	

expansion coefficient of solder alloys between 25 and 150°C was measured by Setsys® TMA with a heating rate of 1°C/min.

Samples of 10 g master alloys were prepared from high purity element pellets (>99.9 wt%) by vacuum arc remelting with the operation voltage of 60 V and 70–80 A. The master alloys were vacuum arc remelted at least three times in order to avoid inhomogeneity of the solder alloy, and the total weight loss of final master alloy was less than 1 wt%. An ultrasonic bath using acetone as the solvent was used to clean samples prior to soldering. 0.15 g master alloys were used in all soldering processes. Furnace soldering was performed in a vacuum of 5×10^{-2} torr at 230°C for 20 minutes. Fig. 2 displays the thermal cycle of Sn-Bi-Ag-(In) solders, the specimen was furnace cooled after holding at 230°C for 20 minutes. To evaluate the microstructural evolution of the solder alloys and the interfacial reaction kinetics for various aging conditions, an oil bath furnace was applied for long-time reliability test. Selected specimens were encapsulated in a glass container and placed into the oil bath furnace kept at 90°C. The specimen was examined after various time periods aging.

The soldered specimens were cut by a low speed diamond saw. Its cross section was first polished by SiC paper, and subsequently polished by 0.3 and 0.05 μm alumina. 2 g $FeCl_3 + 30$ ml $H_2O + 5$ ml $HCl + 60$ ml C_2H_5OH etching solution was used for metallographic examination of Sn-Bi-Ag-(In) solders. The polished cross section of the specimens was examined using a Hitachi 3500 H scanning electron microscope (SEM), and quantitative chemical analysis was performed

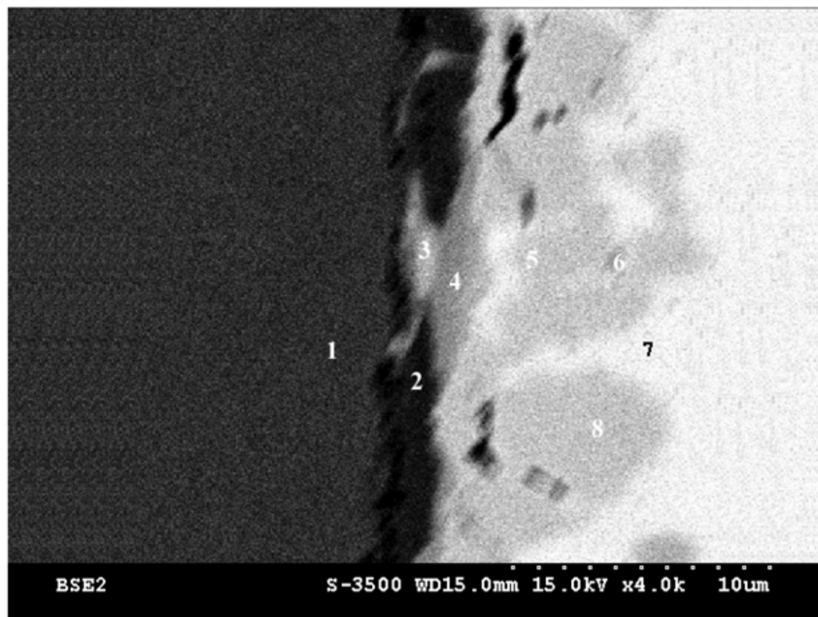

	1		2		3		4		5		6		7		8	
	Wt%	At%	Wt%	At%	Wt%	At%	Wt%	At%	Wt%	At%	Wt%	At%	Wt%	At%	Wt%	At%
Sn	0.0	0.0	0.4	0.2	43.8	25.8	49.6	29.5	91.8	85.5	72.8	57.3	98.6	98.1	73.1	57.5
Ag	0.0	0.0	0.0	0.0	0.1	0.1	0.0	0.0	0.0	0.0	0.0	0.0	0.0	0.0	0.0	0.0
Bi	0.0	0.0	0.0	0.0	0.1	0.0	0.1	0.0	0.5	0.3	0.0	0.0	0.6	0.3	0.0	0.0
In	0.0	0.0	0.0	0.0	0.0	0.0	0.0	0.0	0.0	0.0	0.0	0.0	0.0	0.0	0.0	0.0
Cu	99.4	99.3	3.2	2.6	6.2	6.8	1.7	1.9	2.7	4.7	5.6	8.2	0.5	1.0	3.2	4.7
P	0.0	0.1	17.3	28.6	7.2	16.3	9.4	21.5	0.1	0.5	0.0	0.0	0.0	0.0	0.0	0.0
Ni	0.6	0.6	79.1	68.7	42.7	51.0	39.2	47.1	4.8	9.1	21.7	34.5	0.3	0.5	23.8	37.8

Figure 5 SEM BSE image and EPMA chemical analysis at 94Sn-3Bi-3Ag/substrate interface after soldering at 230°C for 20 minutes.

using a JEOL JXA-8900R electron probe microanalyzer (EPMA). All samples were carbon coated before EPMA analysis.

3. Results and discussion

3.1. Thermal analysis of Sn-Bi-Ag-(In) solders

Table I summarizes the DSC analysis results of selected Sn-Bi-Ag-(In) solders upon heating thermal cycles. It is reported that some degree of undercooling was observed for Sn-based solders, so heating cycle in the DSC analysis was chosen in the melting behavior study [34]. For an off-eutectic alloy, the melting of the alloy starts from solidus temperature (T_s), and completes in liquidus temperature (T_L) [34]. The liquidus temperatures of Sn-(1–5)Bi-(2–3.5)Ag-(0–10)In solders are between 201.7 and 225.3°C, which were higher than that of the most popular eutectic Pb-Sn solder (183°C). It is also noted that the addition of (5–10) wt% In into Sn-Bi-Ag

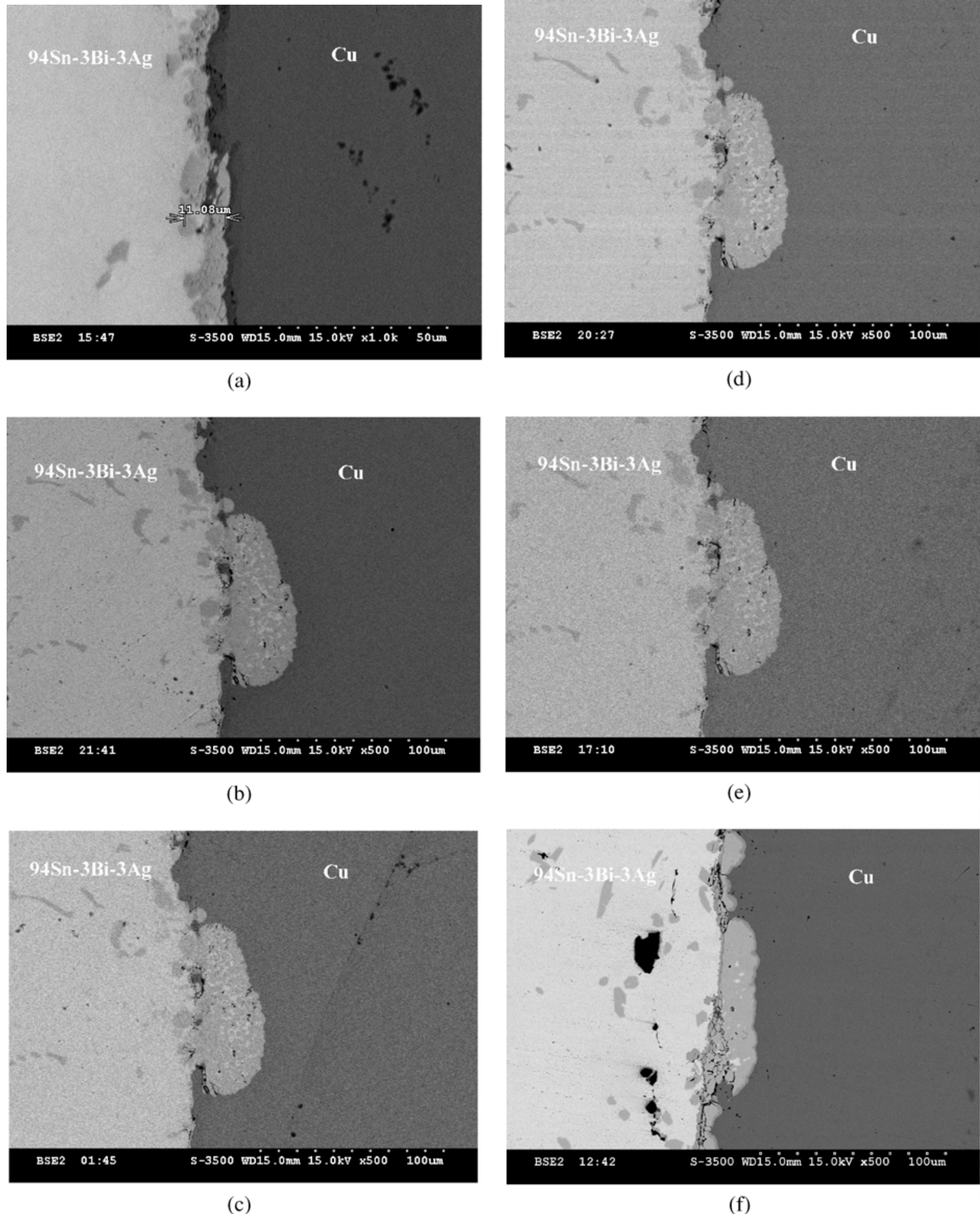

Figure 6 SEM BSE images at 94Sn-3Bi-3Ag/substrate interface after soldering at 230°C for 20 minutes and subsequently aging at 90°C for (a) 7 days, (b) 14 days, (c) 21 days, (d) 28 days, (e) 37 days and (f) 45 days.

solders can effectively decrease the melting point of the alloy.

Fig. 3 shows the endothermic profiles of selected Sn-Bi-(Ag)-(In) solders in DSC analysis. It is important to note that the gap between T_s and T_L temperatures increases with the additions of Bi and In into Sn-Bi-(Ag)-(In) solders. It is highly preferred that the difference between solidus and liquidus temperatures of solder alloys is decreased in order to avoid liquation during soldering [1, 2]. For an alloy with different solidus and liquidus temperatures, the composition of the melt will gradually change as the temperature increases from the solidus to liquidus [1, 2]. If the portion that melts first is allowed to flow out, the remaining solid may not melt and may remain behind as a residue, which is called liquation. Alloys with narrow melting ranges do not tend to liquation, but an alloy with a wide melting range needs rapid heating cycles to minimize phase separation during soldering. It is clear that both (1–5) wt% Bi and (2.5–10) wt% In additions into the Sn-Bi-Ag-In alloys are still far away from the binary eutectic composition as shown in Fig. 4a and b [35]. Phase separation may become a potential problem for such solder alloys with off-eutectic composition.

Table II displays wetting angle measurements of selected Sn-Bi-Ag-(In) specimens soldering at 230°C for 20 minutes on the Au/Ni metallized copper substrate. Although there is no flux applied during soldering, most alloys can still well bond the substrate as shown in the table. There are only four alloys available in Table II, including: 94Sn-3Bi-3Ag, 90Sn-2Bi-3Ag-5In, 81.5Sn-5Bi-3.5Ag-10In and 87Sn-5Bi-3Ag-5In. The wetting angle of 81.5Sn-5Bi-3.5Ag-10In is the largest among all solders. Liquation is observed for 87Sn-5Bi-3Ag-5In alloy, and phase separation may deteriorate its potential application. Therefore, both 94Sn-3Bi-3Ag

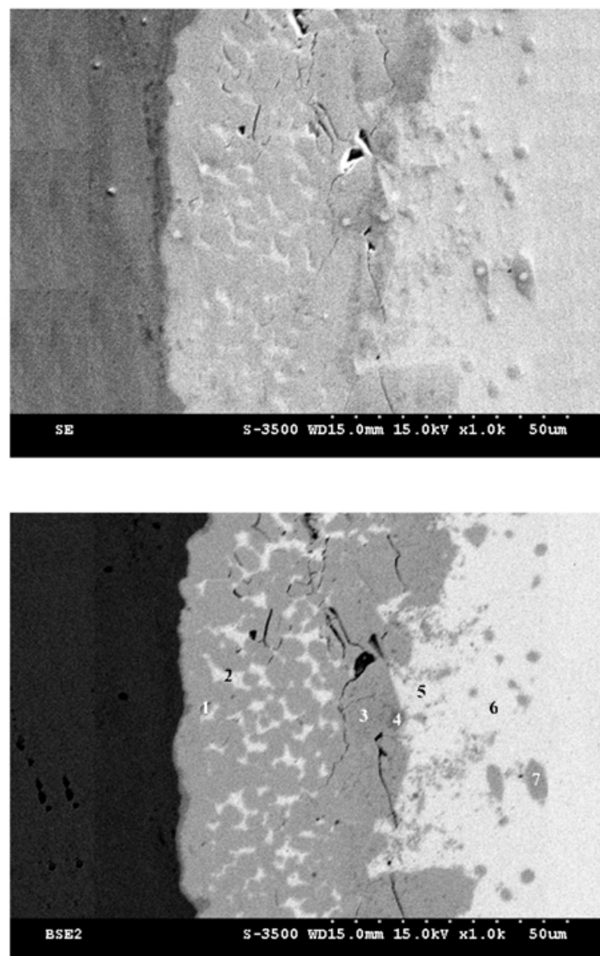

	1		2		3		4		5		6		7	
	Wt%	At%	Wt%	At%	Wt%	At%	Wt%	At%	Wt%	At%	Wt%	At%	Wt%	At%
Sn	60.1	44.6	94.2	93.6	62.4	46.6	62.4	46.2	94.5	93.2	96.8	97.9	63.9	48.4
Ag	0.1	0.1	0.0	0.0	0.0	0.0	0.0	0.0	0.0	0.0	0.0	0.0	0.1	0.1
Bi	0.0	0.0	3.3	1.9	0.0	0.0	0.0	0.0	3.0	1.6	3.0	1.7	0.0	0.0
Ni	2.6	3.8	0.1	0.1	8.4	12.7	15.1	22.7	2.1	4.2	0.1	0.2	6.8	10.4
Cu	37.2	51.5	2.4	4.4	29.2	40.7	22.4	31.1	0.5	0.9	0.1	0.2	29.1	41.1

Figure 7 SEM images and EPMA chemical analysis at the 94Sn-3Bi-3Ag/substrate interface after soldering at 230°C for 20 minutes and subsequently aging at 90°C for 52 days.

and 90Sn-2Bi-3Ag-5In alloys are chosen for further study.

Table III shows the coefficients of thermal expansion (CTEs) of three solder alloys, 94Sn-3Bi-3Ag, 90Sn-2Bi-3Ag-5In and eutectic Sn-Pb. CTEs of both 94Sn-3Bi-3Ag and 90Sn-2Bi-3Ag-5In are slightly less than that of 63Sn-37Pb. Since the CTE of a Si chip is as low as 2.6 ppm/°C at room temperature, the solder alloy with a lower CTE has advantages in electronic packaging due to less residual thermal stress in the packaging after soldering [22]. According to this criterion, 94Sn-3Bi-3Ag and 90Sn-2Bi-3Ag-5In solders are comparable to 63Sn-37Pb solders.

3.2. The stability of 94Sn-3Bi-3Ag/substrate interface in aging

Fig. 5 shows the SEM backscattered electron image and EPMA chemical analysis of 94Sn-3Bi-3Ag after soldering at 230°C for 20 minutes. Point 1 in the figure displays the Cu substrate, and point 2 demonstrates the location of electroless plated Ni layer. It is also noted that the electroless Ni layer contains phosphorus. There are still at least three phases near the interface except the electroless Ni layer, including a Ni-Sn-P phase alloyed with Cu (points 3 and 4), Sn alloyed with minor Cu, Ni and Bi (points 5 and 7), and a Ni-Sn phase alloyed with copper (points 6 and 8). It is reasonable that the location of Ni-Sn-P phase is very close to the interface compared to Sn and Ni-Sn phases. According to the Ni-Sn binary alloy phase diagram shown in Fig. 4c, three Ni-Sn Intermetallics, Ni_3Sn, Ni_3Sn_2 and Ni_3Sn_4, can be observed [35]. The stoichiometric ratio between Ni and Sn content in the Ni-Sn-P ternary compound is close to Ni_3Sn_2. Moreover, the stoichiometry ratio in the Ni-Sn phases can be identified as $(Ni,Cu)_3Sn_4$.

It is observed that the electroless Ni layer is not continuous anymore, and part of the layer has disappeared as shown in the Fig. 5 (point 3). The electroless Ni layer acted as a barrier layer, which can isolate the solder alloy and copper substrate. With the above soldered specimen aging at 90°C, the stability of the electroless Ni layer is greatly impaired. Fig. 6 displays the SEM backscattered electron images at an 94Sn-3Bi-3Ag/substrate interface after soldering at 230°C for 20 minutes and subsequently aging at 90°C for 7, 14, 21, 28, 37 and 45 days, respectively. After 14 days aging at 90°C, some location of the electroless Ni layer break down, and new phases form near the interface. The growth of the new phases is not prominent, and their size remains about the same as the aging time increases from 14 to 45 days. However, the disappearance of the

	1		2		3		4		5		6		7		8	
	Wt%	At%	Wt%	At%	Wt%	At%	Wt%	At%	Wt%	At%	Wt%	At%	Wt%	At%	Wt%	At%
Sn	0.0	0.0	0.2	0.1	0.2	0.1	0.1	0.1	73.1	57.7	78.1	64.5	95.6	95.0	72.2	56.4
Ag	0.0	0.0	0.0	0.0	0.0	0.0	0.1	0.0	0.0	0.0	0.0	0.0	0.0	0.0	0.0	0.0
Bi	0.0	0.0	0.0	0.0	0.0	0.0	0.0	0.0	0.0	0.0	0.1	0.0	0.5	0.3	0.0	0.0
In	0.0	0.0	0.0	0.0	0.0	0.0	0.0	0.0	0.5	0.4	0.9	0.8	3.1	3.2	0.0	0.0
Cu	99.3	99.2	98.6	98.5	1.4	1.2	1.0	0.9	2.1	3.1	1.7	2.7	0.4	0.8	3.8	5.6
P	0.0	0.1	0.0	0.1	7.6	13.5	7.8	13.9	0.0	0.1	0.0	0.0	0.0	0.0	0.0	0.0
Ni	0.7	0.7	1.2	1.3	90.9	85.2	91.0	85.2	24.3	38.7	19.2	32.0	0.3	0.7	24.0	38.0

Figure 8 SEM BSE image and EPMA chemical analysis at 90Sn-2Bi-3Ag-5In/substrate interface after soldering at 230°C for 20 minutes.

electroless Ni layer is still in progress. Fig. 6f shows the interface of the soldered specimen aged at 90°C for 45 days. Its location is different from that of Fig. 4b–e. The electroless Ni layer has almost completely disappeared. The break down of the Ni barrier layer is not simultaneously but gradually in progress.

Fig. 7 shows the SEM images and EPMA chemical analysis at the 94Sn-3Bi-3Ag/substrate interface after soldering at 230°C for 20 minutes and subsequently aging at 90°C for 52 days. The top micrograph is the secondary electron (SE) image, and the second micrograph is the backscattered electron (BSE) image. The SE image demonstrates the topographic image of the observed surface, but the BSE image primarily shows the element distribution in the joint [36, 37]. The left side of the micrographs is the Cu substrate, and the right side of the micrograph is the solder alloy. According to the figure, there is no electroless Ni layer at the interface. Some cracks are observed in the central reaction layer. It is also noted that at least two phases

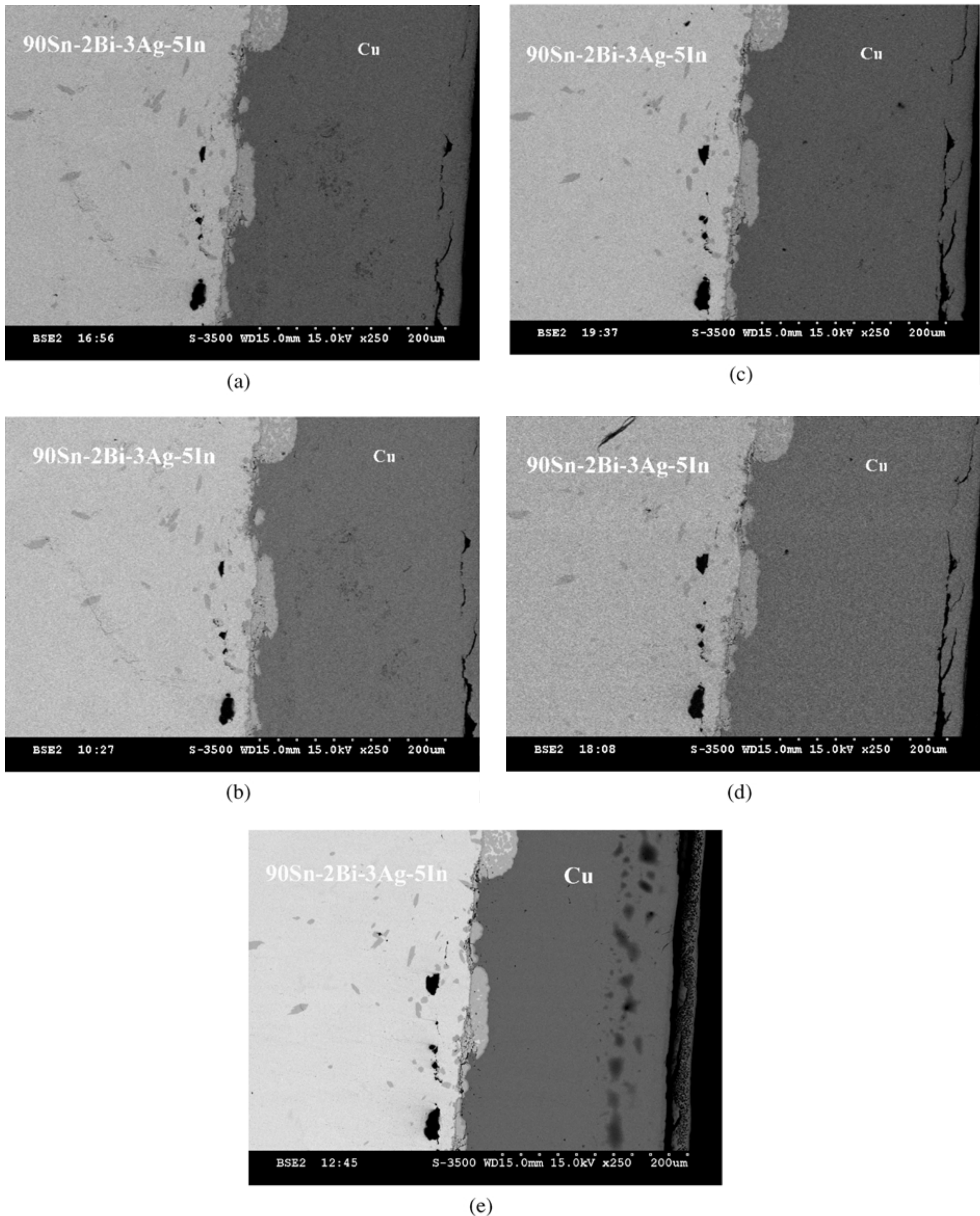

Figure 9 SEM BSE images at 90Sn-2Bi-3Ag-5In/substrate interface after soldering at 230°C for 20 minutes and subsequently aging at 90°C for (a) 14 days, (b) 22 days, (c) 29 days, (d) 38 days and (e) 46 days.

can be identified at the interface. One is Sn alloyed with minor Bi, Ni and Cu (points 2, 5 and 6 in Fig. 7). The other is a Sn-Cu-Ni phase (points 1, 3, 4 and 7 in Fig. 7), which is different from the observations in Fig. 5. Compared with previous $(Ni,Cu)_3Sn_4$ phase in Fig. 5, the copper content in the Sn-Cu-Ni phase is greatly increased. Huge amounts of Cu are dissolved from copper substrate into the interfacial reaction layer. Fig. 4d displays the Cu-Sn binary alloy phase diagram, and the chemical content of η' phase (Cu_6Sn_5) is about 45 at.% Sn [30, 31, 38]. Meanwhile, the stoichiometry of the experimentally observed Sn-Cu-Ni phase is close to $(Cu,Ni)_6Sn_5$. It is well-known that Cu and Ni are completely miscible in solid state [35]. Therefore, it is reasonable to deduce that the interfacial reaction layer is identified as a $(Cu,Ni)_6Sn_5$ phase. It is consistent with literature results that the activation energy for the growth of Cu_6Sn_5 is substantially lower than that for Ni_3Sn_4 [30, 31]. Consequently, the growth of Cu_6Sn_5 is much faster than that of Ni_3Sn_4. Based on experimental results it is clear that, the growth of $(Cu,Ni)_6Sn_5$ phase will dominate the reaction layer for specimens aged at 90°C for long time period.

3.3. The stability of 90Sn-2Bi-3Ag-5In/substrate interface in aging

Fig. 8 shows the SEM backscattered electron image and EPMA chemical analysis at 90Sn-2Bi-3Ag-5In/substrate interface after soldering at 230°C for 20 minutes. The phases nearby the interface are similar to those of 94Sn-3Bi-3Ag. Points 1 and 2 in the figure are primary Cu substrate alloyed with minor Sn, P and Ni. Points 3 and 4 are the electroless Ni layer

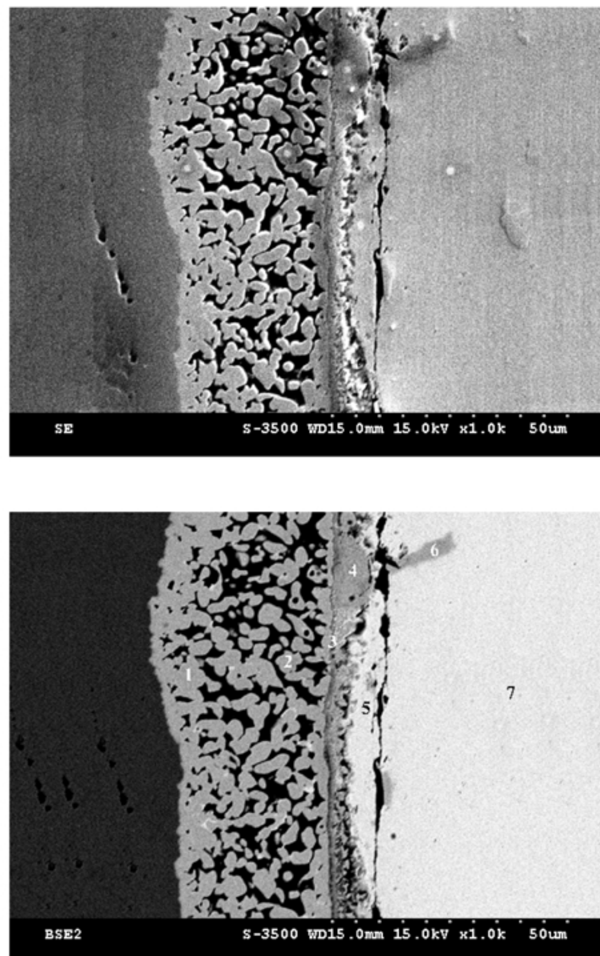

	1		2		3		4		5		6		7	
	Wt%	At%	Wt%	At%	Wt%	At%	Wt%	At%	Wt%	At%	Wt%	At%	Wt%	At%
Sn	58.5	43.4	60.7	45.4	63.6	48.1	59.9	43.7	95.1	95.4	61.9	45.8	95.3	95.8
Ag	0.1	0.1	0.1	0.1	0.2	0.1	0.1	0.1	0.0	0.0	0.1	0.1	0.1	0.1
Bi	0.0	0.0	0.0	0.0	0.1	0.1	0.0	0.0	1.6	0.9	0.0	0.0	1.5	0.9
Ni	2.9	4.4	4.8	7.2	10.2	15.6	16.2	23.9	0.2	0.4	14.5	21.7	0.0	0.0
Cu	36.5	50.7	33.0	46.2	25.2	35.6	23.7	32.2	0.2	0.3	23.3	32.2	0.0	0.0
In	1.9	1.5	1.4	1.1	0.7	0.6	0.2	0.1	3.0	3.1	0.3	0.2	3.1	3.2

Figure 10 SEM images and EPMA chemical analysis at the 90Sn-2Bi-3Ag-5In/substrate interface after soldering at 230°C for 20 minutes and subsequently aging at 90°C for 52 days.

between solder and Cu substrate. Point 7 is mainly comprised of Sn alloyed with minor In, Bi, Cu and Ni. The chemical composition of points 5, 6 and 8 is close to $(Ni,Cu)_3Sn_4$. Fig. 9 displays the SEM BSE images at 90Sn-2Bi-3Ag-5In/substrate interface after soldering at 230°C for 20 minutes and subsequently aging at 90°C for 14 days, 22 days, 29 days, 38 days and 46 days. Similar to previous observations, some locations of the electroless Ni layer are broken down after 14 days aging at 90°C. New phase(s) is (are) formed nearby the interface. The growth of the new phase(s) is not prominent, and its size is kept about the same as the aging time increases from 14 to 46 days. The breakdown of the Ni barrier layer does not occur abruptly but gradually.

Fig. 10 shows the SEM images and EPMA chemical analysis at the 90Sn-2Bi-3Ag-5In/substrate interface after soldering at 230°C for 20 minutes and subsequently aging at 90°C for 52 days. The width of the reaction layer is approximately 40 μm. According to its EPMA chemical analysis, the reaction layer is mainly comprised of $(Cu,Ni)_6Sn_5$ phase. It is also noted that there are lots of voids in the reaction layer, so the growth of $(Cu,Ni)_6Sn_5$ phase at the interface is detrimental to the bonding between solder and substrate.

4. Conclusions

1. The liquidus temperatures of Sn-(1–5)Bi-(2–3.5) Ag-(0–10)In solders are between 201.7 and 225.3°C, which are higher than that of the most popular eutectic Pb-Sn solder (183°C). Additions of (5–10) wt% In into Sn-Bi-Ag solders can effectively decrease the melting point of the solder alloy. However, the gap between T_s and T_L temperatures increases with the additions of Bi and In into Sn-Bi-Ag-(In) solders.

2. Although there is no flux applied in the experiment, most Sn-Bi-Ag-(In) solder alloys can well bond the Au/Ni metallized copper substrate. 94Sn-3Bi-3Ag solder demonstrates the lowest wetting angle of 45° among all test samples.

3. Thermal expansion coefficients of both 94Sn-3Bi-3Ag and 90Sn-2Bi-3Ag-5In are slightly less than that of 63Sn-37Pb.

4. Both 90Sn-2Bi-3Ag-5In/substrate and 94Sn-3Bi-3Ag/substrate interfaces demonstrate similar reaction kinetics in the experiment. The stability of the interface is greatly impaired during 90°C aging. Some locations of the electroless Ni layer break down, and new phases are formed nearby the interface in aging treatment. Initially, the growth of Ni-rich $(Ni,Cu)_3Sn_4$ phase dominates the interfacial reaction. However, the growth of Cu-rich $(Cu,Ni)_6Sn_5$ phase will dominate the reaction layer for specimens aged at 90°C for long time periods.

Acknowledgements

The authors gratefully acknowledge the financial support for this study by the National Science Council (NSC), Republic of China under NSC Grant 90-2216-E-259-003.

References

1. G. HUMPSTON and D. M. JACOBSON, "Principles of Soldering and Brazing" (ASM International, Ohio, 1993) p. 1.
2. M. M. SCHWARTZ, "Brazing: For the Engineering Technologist" (ASM International, Ohio, 1987) p. 1.
3. D. L. OLSON, T. A. SIEWERT, S. LIU and G. R. EDWARDS, "ASM Handbook, Welding, Brazing, and Soldering" Vol. 6 (ASM International, Ohio, 1993) p. 109.
4. M. M. SCHWARTZ, "Ceramic Joining" (ASM International, Ohio, 1990) p. 1.
5. M. ABTEW and G. SELVADURAY, *Mater. Sci. Eng.* R. **27** (2000) 95.
6. D. GUPTA, K. VIEREGGE and W. GUST, *Acta Mater.* **47** (1999) 5.
7. V. STOLKARTS, L. M. KEER and M. E. FINE, *J. Mech. Phys. Solids* **47** (1999) 2451.
8. P. M. BUECHNER, D. STONE and R. S. LAKES, *Scripta Mater.* **41** (1999) 561.
9. T. K. HA and Y. W. CHANG, *ibid.* **40** (1999) 103.
10. W. DREYER and W. H. MULLER, *Int. J. Solids and Structures* **37** (2000) 3841.
11. W. W. LEE, L. T. NGUYEN and G. S. SELVADURAY, *Microelectron. Reliab.* **40** (2000) 231.
12. Y. C. CHAN, P. L. TU, A. C. K. SO and J. K. L. LAI, *IEEE T. Compon. Pack.* B **20** (1997) 463.
13. J. GLAZER, *Int. Mater. Rev.* **40** (1995) 65.
14. M. L. HUANG, C. M. L. WU and J. K. L. LAI, *J. Mater. Sci.-Mater. El.* **11** (2000) 57.
15. T. LAINE-YLIJOKI, H. STEEN and A. FORSTEN, *IEEE T. Compon. Pack.* C **20** (1997) 194.
16. V. I. IGOSHEV, J. I. KLEIMAN, D. SHANGGUAN, C. LOCK and S. WONG, *J. Electron. Mater.* **27** (1998) 1367.
17. C. S. OH, J. H. SHIM, B. J. LEE and D. N. LEE, *J. Alloy. Compd.* **238** (1996) 155.
18. C. G. SCHMIDT, J. W. SIMONS, C. H. KANAZAWA and D. C. ERLICH, *Microelectron. Reliab.* **37** (1997) 536.
19. D. J. XIE, *ibid.* **40** (2000) 1191.
20. T. TAEKOO, J. JINHYUK and I. JUNG, *ibid.* **38** (1998) 1941.
21. R. DARVEAUX, J. HECKMAN, S. JIM, M. AHMER and S. ANDREW, *ibid.* **40** (2000) 1117.
22. W. D. ZHUANG, P. C. CHANG, F. Y. CHOU and R. K. SHIUE, *ibid.* **41** (2001) 2011.
23. S. VAYNMAN and M. E. FINE, *Scripta Mater.* **41** (1999) 1269.
24. A. M. MINOR and J. W. MORRIS JR., *J. Electron. Mater.* **29** (2000) 1170.
25. C. E. HO, R. ZHENG, G. L. LUO, A. H. LIN and C. R. KAO, *ibid.* **29** (2000) 1175.
26. T. M. KORHONEN, P. SU, S. J. HONG, M. A. KORHONEN and C. Y. LI, *ibid.* **29** (2000) 1194.
27. K. C. HUNG, Y. C. CHAN, H. C. ONG, P. L. TU and C. W. TANG, *Mat. Sci. Eng. B: Solid* B **76** (2000) 87.
28. K. W. MOON, W. J. BOETTINGER, U. R. KATTNER, C. A. HANDWERKER and D. J. LEE, *J. Electron. Mater.* **30** (2001) 45.
29. X. QIAO and S. F. CORBIN, *Mater. Sci. Eng. A: Struct.* A **283** (2000) 38.
30. C. CHEN, C. E. HO, A. H. LIN, G. L. LUO and C. R. KAO, *J. Electron. Mater.* **29** (2000) 1200.
31. M. L. HUANG, C. M. L. WU, J. K. L. LAI and Y. C. CHAN, *ibid.* **29** (2000) 1021.
32. C. M. L. WU, M. L. HUANG, J. K. L. LAI and Y. C. CHAN, *ibid.* **29** (2000) 1015.
33. J. P. SIBILIA, "Materials Characterization and Chemical Analysis" (VCH Publishers Inc., New York, 1996) p. 261.
34. S. W. YOON, J. R. SOH, H. M. LEE and B. J. LEE, *Acta Mater.* **45** (1997) 951.
35. T. B. MASSALSKI, "Binary Alloy Phase Diagrams" (ASM International, Ohio, 1990).
36. R. E. LEE, "Scanning Electron Microscopy and X-Ray Microanalysis" (Prentice Hall, New York, 1993) p. 130.
37. C. C. LIU, C. L. OU and R. K. SHIUE, *J. Mater. Sci.*, **37** (2002) 2225.
38. S. W. YOON, W. K. CHOI and H. M. LEE, *Scripta Mater.* **40** (1999) 327.

Received 12 March
and accepted 24 December 2002